

Increasing the Maximum Achievable Strain of a Covalent Polymer Gel Through the Addition of Mechanically Invisible Cross-Links

Zachary S. Kean, Jennifer L. Hawk, Shaoting Lin, Xuanhe Zhao, Rint P. Sijbesma, and Stephen L. Craig*

Polymer organogels and hydrogels are important materials for applications ranging from biomedical implants and tissue engineering^[1] to soft, active devices. For many of these applications, a high range of motion (i.e., achieving high strains) is desirable, but the network defects of polymer gels often limit the maximum strain they can achieve.^[2,3] Many biological and device applications would benefit from gels that withstand high strains without having to pay the energetic costs associated with added, highly dissipative interactions in current stretchable gels.^[4–6] Structurally homogeneous “precision” networks constructed from monodisperse molecular elements have been proposed to result in a smooth network stress distribution^[12] that can accommodate high strains^[7,8] with minimal energy dissipation.^[9–11] This approach, however, typically cannot be transferred to existing gels made from easily accessible random biopolymer or synthetic polymer networks. An ideal solution would be to identify modifications that have no discernable impact on the modulus of a gel and maintain high levels of elastic recovery, while permitting the gel to achieve otherwise inaccessible strains repeatedly over multiple loading cycles without a loss in mechanical properties. Here we show that the addition of transient, supramolecular cross-links to a covalent polymer gel can provide dramatic increases in the maximum achievable strain at break, even when the added supramolecular cross-links are so weak and dynamic as to be effectively invisible in terms of their contribution to modulus or energy dissipation in the materials under their loading environment. The results suggest that classes of “very weak” supramolecular interactions might play an important, previously overlooked, role in developing next generation gels.

Model organogels were synthesized by reaction of poly(4-vinylpyridine) (P4VP) with a dibromide functional crosslinker in DMSO (Figure 1a). The P4VP has an M_n of 33 kDa and a polydispersity of 1.35 (see methods section), and cross-linking was introduced by selectively alkylating a small fraction of the pyridine groups along the polymer backbone (~315 average repeat units), resulting in a heterogeneous network mesh. Cross-linking with 1,6-dibromohexane (1 per 50 pyridines) led to network PN1, which was subsequently punched into cylinders and swollen to equilibrium in DMSO (polymer volume fraction $\phi \sim 0.03$). The fragile nature of the nascent PN1 gels necessitated the use of unconfined uniaxial compression (hereafter compression) for the majority of our characterization. Consistency in the compression results was achieved by restricting studies to low strain values (<0.8)^[14] and maintaining proper sample geometry to avoid buckling.^[15] The failure point from the stress-strain curves was validated through the use of a chemiluminescent probe (see below). Weak, transient supramolecular cross-links were introduced into the PN1 network by immersing the PN1 cylinders in 5 mM DMSO solutions of bifunctional van Koten-type^[16] pincer complexes, which coordinate reversibly on either end to free pyridines along the polymer side chain. The stoichiometry is such that at 5 mM pincer, full uptake would give roughly 5 times as many reversible cross-linkers as covalent cross-linkers. Mechanical testing (see Figure 2, below) shows that the number of reversible cross-linkers introduced in this way is comparable to the number of covalent cross-linkers, consistent with the concentrations and associations constants of the pincer complexes. The pincers were chosen because they are versatile probes of dynamic molecular contributions to bulk macromolecular properties;^[17–20] small structural changes in the metal and ligand adjust the lifetime of the cross-linker across a range from milliseconds to minutes. This control element is critical for our strategy,^[13] as it provides access to hybrid gels in which the reversible component rearranges so rapidly that it makes a negligible contribution to the compressive mechanical properties on typical experimental timescales.

The consequences of the weak cross-linking on hybrid gel properties are shown in Figure 2. When PN1 is compressed rapidly ($\sim 8 \text{ mm s}^{-1}$, 4 s^{-1}) to 20% strain and held for 1 s, the stress is stored in its covalent network, and minimal relaxation is observed.^[21] When the PdEt cross-linker ($t_{1/2} = 41 \text{ ms}$; “fast”) is added, some additional stress is stored in the reversible cross-linker, and that stress dissipates over a few tenths of seconds. The even more rapidly dissociating PdMe ($t_{1/2} = 0.48 \text{ ms}$, “faster”) accumulates even less additional energy. When the

Z. S. Kean, J. L. Hawk, Prof. S. L. Craig
Department of Chemistry
Duke University
Durham, NC 27708–0346, USA
E-mail: stephen.craig@duke.edu



S. Lin, Prof. X. Zhao
Soft Active Materials Lab
Department of Mechanical Engineering and Materials Science
Duke University
Durham, NC 27708, USA
Prof. R. P. Sijbesma
Laboratory of Macromolecular and Organic Chemistry and the Institute
for Complex Molecular Systems
Eindhoven University of Technology
Eindhoven, The Netherlands

DOI: 10.1002/adma.201401570

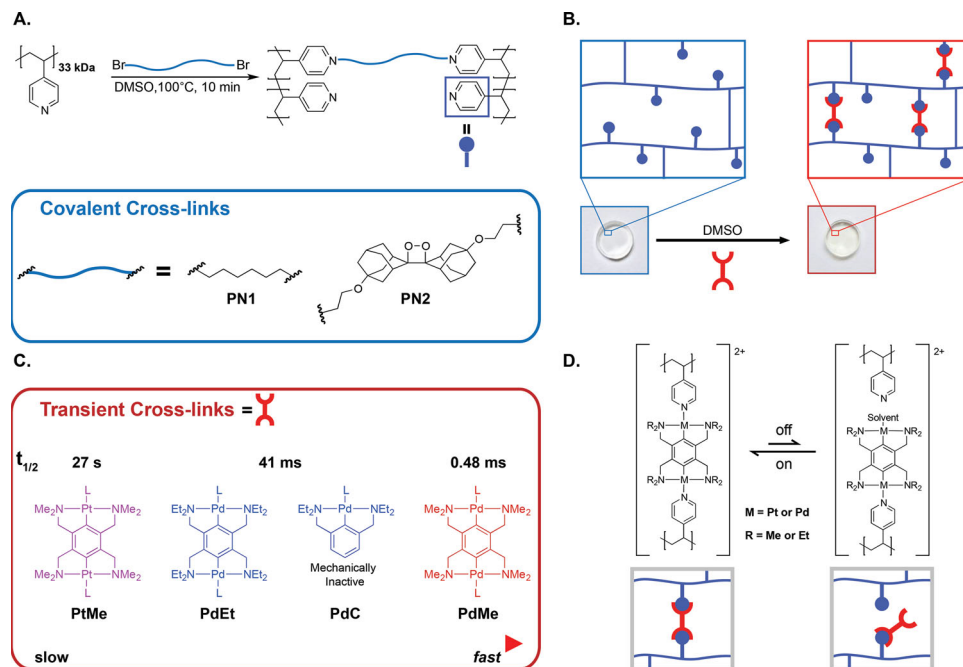


Figure 1. Structure and dynamics of PN organogels. (a) Synthesis of PN1 and PN2 organogels by alkylation of P4VP with dibromide cross-linkers in DMSO. (b) Cylinders (typical diameter = 4.4–5.0 mm, typical height = 1.6–1.8 mm) of covalent organogel PN1 (left) incorporate transient pincer cross-links (right) by coordination with pyridine side-groups (blue circles) in P4VP-based networks (PN1-PdEt [5 mM]) shown. (c) Structure and metal-pyridine half-lives of pincer-based cross-linkers in DMSO (solvent).^[13] (d) Solvent mediates the reversible dissociation of metal-pyridine bonds.

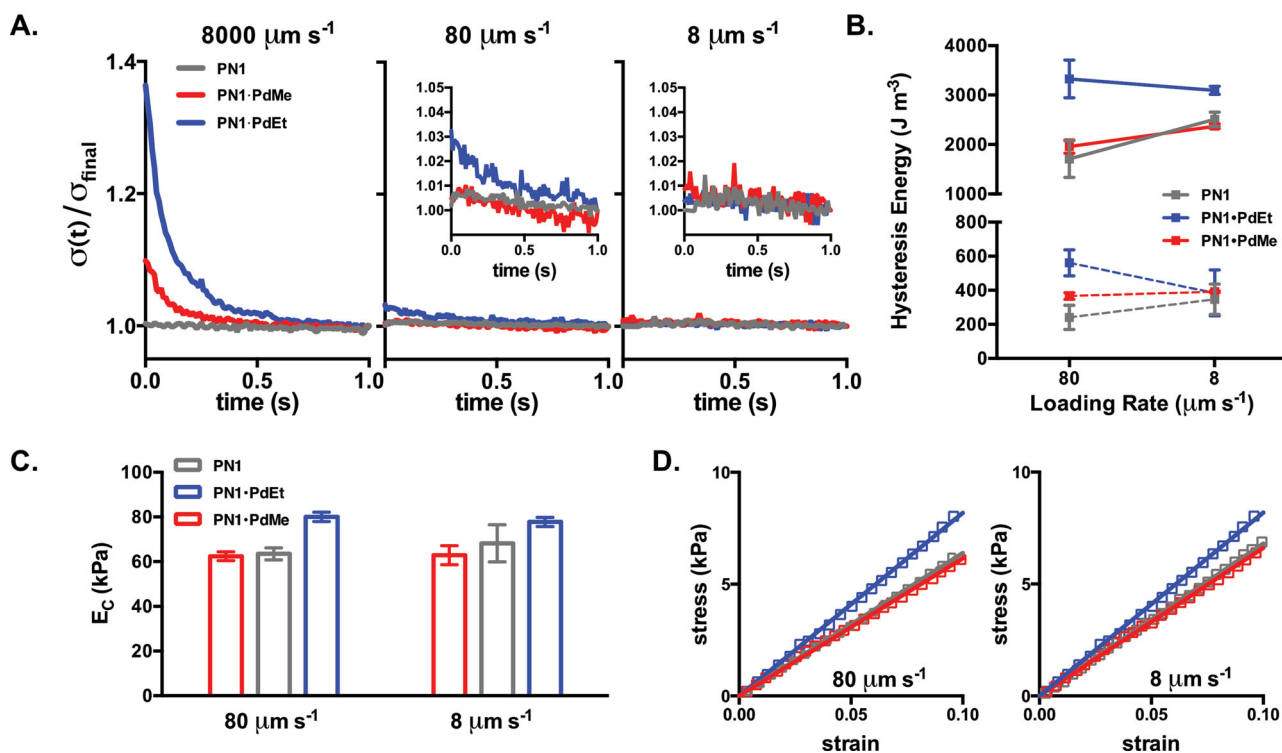


Figure 2. Energy dissipation in hybrid networks. (a) Time-dependent low-strain ($\epsilon = 0.2$) relaxation behavior of PN1 (grey), PN1-PdEt (blue), and PN1-PdMe (red) organogel cylinders showing decreased mechanical activity of pincer cross-links with decreased loading rate. Stress as a function of time after loading ($\sigma(t)$) is normalized by the stress at $t = 1$ s (σ_{final}) and insets show magnified relaxation curves. (b) Hysteresis energy for PN1-based networks under compression ($\epsilon = 0.4$ (solid), 0.2 (hashed)) at different loading rates. (c,d) E_c of PN1-based networks as a function of loading rate, determined by stress-strain curves under compression (squares) and linear fit ($\epsilon = 0-0.1$, solid). PdEt cross-links make minor contributions to E_c while PdMe crosslinks are mechanically “invisible.” Error bars denote SEM, $n = 3$. $T = 25$ °C for all experiments.

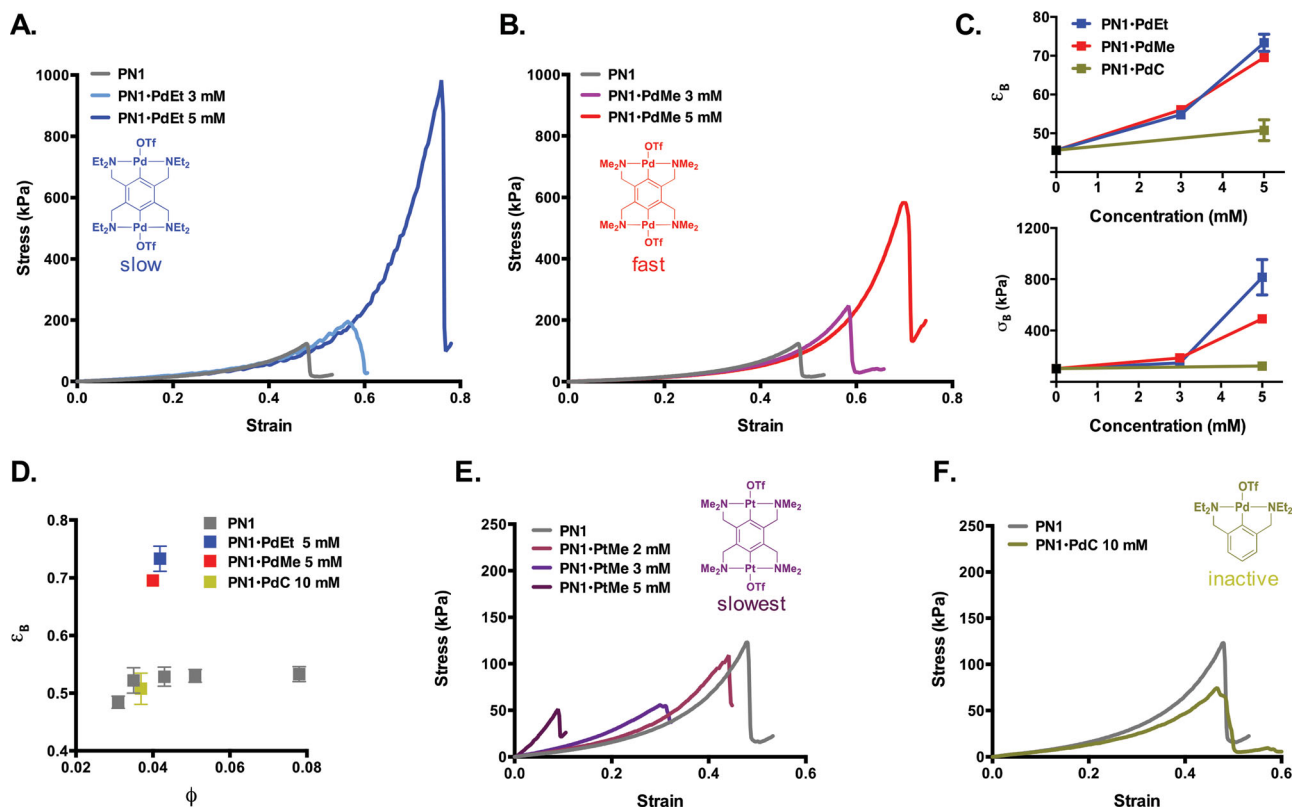


Figure 3. Compression testing of covalent (PN1) and hybrid (PN1-Pd) organogels. (a,b) Representative stress-strain behavior of PN1 (grey), PN1-PdEt (blue), and PN1-PdMe (red) as a function of pincer concentration. (c) Monotonic increases in ϵ_B and σ_B of PN1 network with increasing pincer concentration. (d) Strain at break (ϵ_B) vs. polymer volume fraction (ϕ) showing only minimal change in properties of PN1 due to differential swelling. Error bars denote SEM, $n = 5$. (e) Stress-strain behavior of PN1-PtMe gels bearing the slowest dissociating cross-links. In contrast to the more transient pincers, samples become increasingly brittle with increased PtMe concentration. (f) Representative stress-strain curve showing the effect of added mechanically inactive control pincer PdC. Loading rate = $80 \mu\text{m s}^{-1}$, $T = 25^\circ\text{C}$.

loading rate is reduced to $80 \mu\text{m s}^{-1}$, the amount of additional stress stored in the reversible component of PN1-PdEt drops to $\sim 2\%$, and that stored in the reversible component of PN1-PdMe is too small to be detected. Slowing the compression further to $8 \mu\text{m s}^{-1}$ led to indistinguishable relaxation behavior among the nascent covalent and both hybrid gels.

As expected, therefore, the hybrid networks store minimal additional energy relative to PN1, and subsequent characterization shows that the same is true for the amount of energy dissipated. Stress-strain hysteresis (Figure 2b) reveals that the amount of energy dissipated in PN1-PdEt is measurably larger than that of PN1 at $80 \mu\text{m s}^{-1}$ but not at $8 \mu\text{m s}^{-1}$, while the hysteresis energy of PN1-PdMe is indistinguishable from that of PN1 at both loading rates. Hysteresis energies shown in Figure 2b amount to between 18 and 34% at low strain ($\epsilon = 0.2$) and between 21 and 46% at high strain ($\epsilon = 0.4$, Supporting Table S2). Measurements of compressive moduli (E_C , taken as the initial slope of the stress-strain curves) further confirm that additional energy input is needed to strain “fast” PN1-PdEt relative to PN1 ($E_C = 80$ vs. 64 kPa at $80 \mu\text{m s}^{-1}$). Conversely, the modulus of “fastest” PN1-PdMe (62 kPa) was indistinguishable from that of the parent gel, consistent with the short lifetime of the PdMe cross-linkers relative to the timescale of the

compression. The three gels have the same covalent network, the active chains of which contribute roughly $62\text{--}64 \text{ kPa}$ to the modulus of each system. The supramolecular component of the PN1-PdEt network contributes an additional 25% to the modulus, whereas the contribution of the supramolecular component of PN1-PdMe is too small to be measured. The minimal contributions of these elements are seen as well in low strain oscillatory rheology (Supporting Figure S9).

The overlay of the red (PN1-PdMe) and gray (PN1) data, especially the stress-strain curves in Figure 2d, is particularly compelling. For a given strain, the same energy is being stored in the same covalent framework, and so the behavior of the hybrid networks as the gels were compressed further came as a surprise. The PN1 gels are fairly weak, with an average compressive strain-at-break (ϵ_B) of 0.46, and stress-at-break (σ_B) of 103 kPa at the $80 \mu\text{m s}^{-1}$ loading rate. In comparison, PN1-PdEt showed a dramatic increase in ϵ_B (0.73 vs. 0.46) and σ_B (816 kPa vs. 103 kPa) (Figure 3a), somewhat surprising given the otherwise modest mechanical activity of the transient PdEt cross-linker. Given this result, we then examined the effect of introducing PdMe that, due to increased lability ($t_{1/2} = 0.48 \text{ ms}$) makes no measurable contribution to modulus and bears no measurable stress. Unexpectedly, these hybrid gels

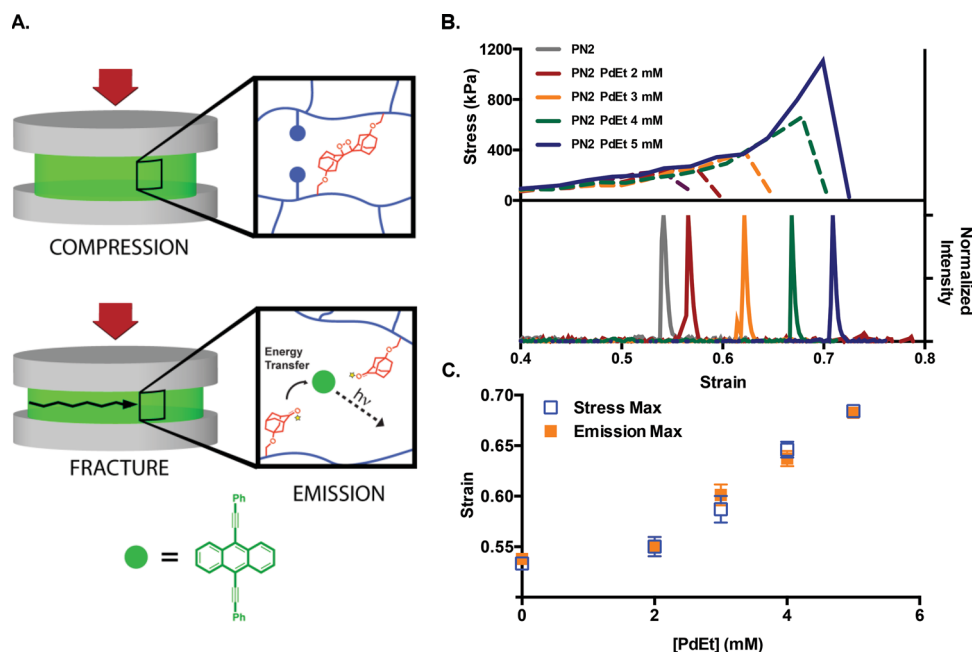


Figure 4. Probing covalent failure with mechanically generated chemiluminescence. (a) **PN2** network structure bearing dioxetane-functional crosslinks. Samples are video recorded under loading in a compression geometry. Photons are emitted upon failure (crack propagation) of the underlying covalent network, allowing for the collection of emission-strain data simultaneously with stress-strain data. (b) Representative stress-strain and emission intensity-strain plots of **PN2-PdEt** gels as a function of **[PdEt]**. (c) Strain at Emission max and stress max vs. **[PdEt]**. Microscopic failure emission max) is observed to occur in concert with macroscopically observe failure (stress max). Error bars denote SEM, $n = 10$. Loading rate = $80 \mu\text{m s}^{-1}$, $T = 25 \text{ }^\circ\text{C}$.

also demonstrated dramatic increases in stress and strain at break ($\epsilon_B = 0.68$, $\sigma_B = 492 \text{ kPa}$; 5 mM PdMe) (Figure 3b).

The observed effect is due to the introduction of dynamic cross-links, as supported by several observations. First, the strain (and stress) at break increases monotonically as a function of **PdEt** or **PdMe** loading (Figure 3c). Second, while some deswelling occurs upon introduction of pincer complexes, the effect of differential swelling was ruled out by compression testing of **PN1** gels swollen to a wide range of polymer volume fractions ($\phi \sim 0.03\text{--}0.08$, varied by addition of co-solvent; see Supporting Figure S4) that encompass those observed in all **PN1-Pd** samples ($\phi \sim 0.03\text{--}0.04$). Differential swelling has only a minimal impact on ultimate properties, relative the impact of added pincer complex (Figure 3d). To ensure that the effect is due to cross-linking rather than simply chemical modification, we introduced the mechanically inactive monofunctional control **PdC** (10 mM , equivalent $[\text{Pd}]$ to 5 mM PdEt). Again, only a minimal effect was observed ($\epsilon_B = 0.51$, $\sigma_B = 122 \text{ kPa}$), consistent with the minor effect of differential swelling (Figures 3d and e). Additional experiments reveal that dynamic rearrangement of the network is required for enhanced ϵ_B in this system; for example, replacing the metal center with platinum increases the cross-linker lifetime by five orders of magnitude (**PtMe** vs. **PdMe**) to $\sim 38 \text{ s}$, which is on the order of the compression experiment ($1\text{--}10 \text{ s}^{-1}$). Though it may be expected that **PN1-PtMe** would display increased ϵ_B with increased E_C , we instead observed diminished ϵ_B (0.07) with increased modulus ($E_C = 354 \text{ kPa}$), reminiscent of increasing the concentration of covalent or strong ionic cross-links (Figure 3f). Based on these observations, it is apparent that rapid dissociation of supramolecular cross-links (**PdMe** and **PdEt**) is required to increase ϵ_B .

To probe directly how the fracture behavior of the underlying covalent network changed as a function of the added supramolecular component, we employed **PN2**. **PN2** bears a bis(adamantyl) dioxetane mechanophore cross-linker, which behaves as a chemiluminescent indicator of covalent failure^[22,23] (Figure 4a). Upon rupture, the dioxetane mechanophore breaks to form electronically excited adamantanone chain ends that rapidly transfer energy to the singlet acceptor 9,10-bis(phenylethynyl) anthracene, which ultimately emits a photon at $\sim 600 \text{ nm}$ (Supporting Movie S1). **PN2-PdEt** was subjected to compression testing at various **PdEt** concentrations, and the emission was simultaneously recorded using a CMOS-based sensor at 33 FPS. As seen in Figure 4b, the onset of emission due to failure of the covalent network shifts in concert with strain at break, while the integral emission intensity and duration of emission remains constant (Supporting Figure S6). The reversible interactions, even when not bearing stress within the network, therefore inhibit the scission of the underlying covalent network that is actively bearing greater stresses in their presence.

Given that the underlying covalent framework survives high strains in the hybrid networks, we examined the elastic recovery of **PN1-Pd** under deformations ($\epsilon = 0.6$) that would be catastrophic for the pure covalent network ($\epsilon_B = 0.46$). In contrast to most dissipative gels reported to date,^[24–26] the enhanced stress/strain at break comes without significant loss upon immediate reloading, as shown in Figure 5. The dissipation in hybrid networks obviously cannot be compared to that of **PN1** at these high strains, but qualitatively we see that the area between the loading (solid color) and unloading (dashed) curves is small, especially for **PN1-PdMe**. While **PN1-PdEt**

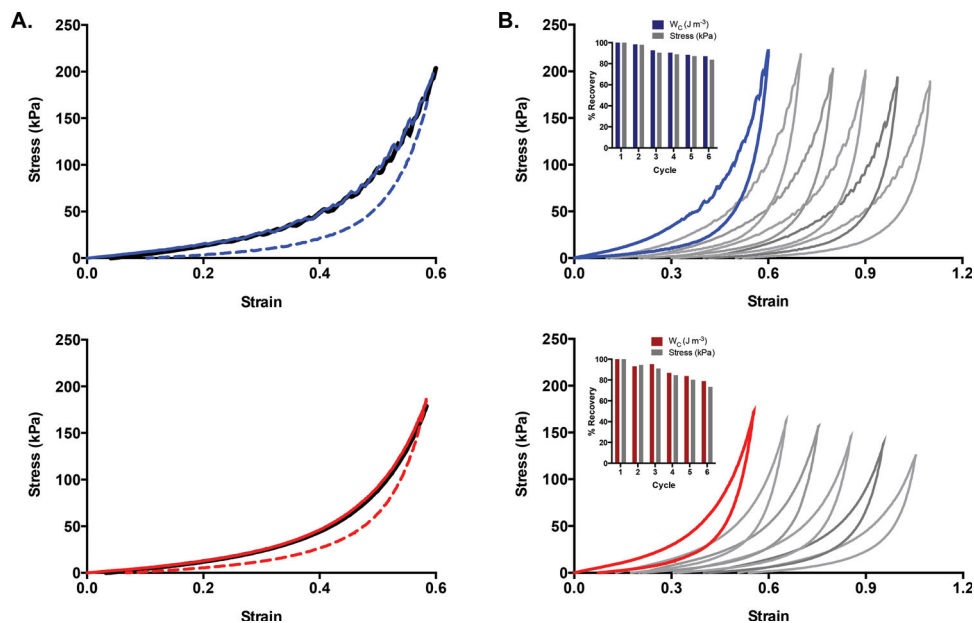


Figure 5. Recovery and cyclic loading in PN1-PdMe and PN1-PdEt gels. (a) Loading (solid, $\epsilon = 0.6$), unloading (dashed), and immediate reloading (black) curves for PN1-PdMe [5 mM] (blue) and PN1-PdEt [5 mM] (red) cylinders under compression. (b) Representative cyclic loading curves ($\epsilon = 0.6$) for PN1-PdMe [5 mM] (blue) and PN1-PdEt [5 mM] (red). Inset shows work of compression (W_c , J m^{-3}) and peak stress (kPa) for each cycle. Strain axis offset for clarity. Loading rate = $80 \mu\text{m s}^{-1}$, $T = 25 \text{ }^\circ\text{C}$.

exhibits consistently higher dissipation, this loss is recoverable, with both systems showing near complete recovery of modulus upon immediate reloading ($\sim 99\%$). Both PN1-PdEt and PN1-PdMe were subjected to instantaneous cyclic loading cycles under compression, comparing the stress reached and work of compression (W_c , J m^{-3}) on each loading cycle. Both recovered $\sim 93\%$ of their W_c after three cycles. At six cycles, PN1-PdEt achieved 87% recovery while PN1-PdMe showed 79%, indicating a slightly higher level of fatigue resistance in the case of PdEt. Increases in ultimate strain are not unknown in systems where added non-covalent cross-links contribute considerably to the stress-bearing properties of the network.^[4,27] It is remarkable though, that the addition of PdMe, which does not contribute to E_c , has such a profound effect on the survivability of the otherwise identical PN1 network. This indicates that these labile non-covalent cross-links are able to prevent network failure under conditions where they bear virtually zero stress.

Here, we have demonstrated that mechanically “invisible” elements can have a profound effect on the stress-strain behavior of an otherwise unremarkable random network. These added dynamic cross-links have a negligible effect on nascent properties and structure, but allow for much greater stress and strain to be borne within the same covalent network that typically fractures at much lower strains. The impact is realized even with transient cross-links that neither store nor dissipate measurable macroscopic stress within the network under the conditions tested. These benefits come from a range of supramolecular interactions that are relatively unexploited in polymers, where the focus has historically been on strong association constants and/or slow dissociation rates.^[27,29–33] Here, cross-linking interactions that are both thermodynamically (association constants $\sim 30 \text{ M}^{-1}$) and kinetically ($t_{1/2} < 1 \text{ ms}$) weak^[13] lead to gels that

are ultimately not only more deformable, but also stronger, than comparable networks formed from stronger and slower interactions (PtMe, 8000 M^{-1} and 27 s , respectively). We speculate that dynamic material properties on the timescale of crack propagation, rather than loading, might be critical, and we observe substantial enhancements in fracture energies that are consistent with this interpretation (PN1 $\sim 1.2 \text{ J m}^{-2}$, PN1-PdEt $\sim 5.7 \text{ J m}^{-2}$, PN1-PdMe $\sim 29.4 \text{ J m}^{-2}$; Supporting Figure S8). Alternatively, the dynamic supramolecular topology might serve to “smooth out” the stress distribution on the molecular level throughout the network, minimizing as a consequence the stress concentrations that initiate crack formation and propagation.^[2,34,35] Regardless of mechanism, however, these results suggest that there might be contributions toward the effects observed when reversible interactions are added to polymer gels for the different objective of increased toughness, which is typically obtained by maximizing energy dissipation as quantified by the hysteresis observed in the loading cycles. Higher strains at break are often observed in such systems,^[4,24,27] and while previously alluded to,^[36,37] the results presented here provide some evidence that the effect often assumed to be tied to the extent of energy dissipation under load might, in fact, have contributions from other mechanisms. The results motivate further study of how polymer networks can be modified in a way that decouples contributions to fracture energy from the contributions to deformation energy (modulus). To that end, the networks presented here, and related systems, might prove useful in developing and testing quantitative relationships. Such modifications have practical implications as well, because in contrast to common approaches, here high strains are achieved without paying additional energy costs to dissipation. This feature is particularly attractive for soft active devices and biomaterials where a high range of motion is required.

Supporting Information

Supporting Information is available from the Wiley Online Library or from the author.

Acknowledgements

We thank A. Crosby and C. Creton for thoughtful discussions. Z.S.K. thanks Y. Chen for helpful discussions and experimental guidance. This material is based on work supported by the NSF (CHE- 1124694) and NSF Triangle MRSEC (DMR-1121107). R.P.S. thanks the Ministry of Education, Culture and Science (Gravity program 024.001.035) for support. X.H.Z. thanks NSF CAREER Award CMMI-1253495 for support.

Received: April 7, 2014

Revised: May 20, 2014

Published online:

- [1] K. Y. Lee, D. J. Mooney, *Chem. Rev.* **2001**, *101*, 1869.
- [2] G. J. Lake, A. G. Thomas, *Proc. R. Soc. London, Ser. A* **1967**, *300*, 108.
- [3] P. Calvert, *Adv. Mater.* **2009**, *21*, 743.
- [4] J.-Y. Sun, X. Zhao, W. R. K. Illeperuma, O. Chaudhuri, K. H. Oh, D. J. Mooney, J. J. Vlassak, Z. Suo, *Nature* **2012**, *489*, 133.
- [5] R. E. Webber, C. Creton, H. R. Brown, J. P. Gong, *Macromolecules* **2007**, *40*, 2919.
- [6] J. P. Gong, Y. Katsuyama, T. Kurokawa, Y. Osada, *Adv. Mater.* **2003**, *15*, 1155.
- [7] M. Malkoch, R. Vestberg, N. Gupta, L. Mespouille, P. Dubois, A. F. Mason, J. L. Hedrick, Q. Liao, C. W. Frank, K. Kingsbury, C. J. Hawker, *Chem. Commun.* **2006**, 2774.
- [8] A. M. Cok, H. Zhou, J. A. Johnson, *Macromol. Symp.* **2013**, *329*, 108.
- [9] J. Cui, M. A. Lackey, A. E. Madkour, E. M. Saffer, D. M. Griffin, S. R. Bhatia, A. J. Crosby, G. N. Tew, *Biomacromolecules* **2012**, *13*, 584.
- [10] T. Sakai, Y. Akagi, T. Matsunaga, M. Kurakazu, U.-i. Chung, M. Shibayama, *Macromol. Rapid Commun.* **2010**, *31*, 1954.
- [11] T. Sakai, T. Matsunaga, Y. Yamamoto, C. Ito, R. Yoshida, S. Suzuki, N. Sasaki, M. Shibayama, U.-i. Chung, *Macromolecules* **2008**, *41*, 5379.
- [12] Y. Okumura, K. Ito, *Adv. Mater.* **2001**, *13*, 485.
- [13] S. L. Jeon, D. M. Loveless, W. C. Yount, S. L. Craig, *Inorg. Chem.* **2006**, *45*, 11060.
- [14] Y. Xiao, E. A. Friis, S. H. Gehrke, M. S. Detamore, *Tissue Eng Part B Rev* **2013**, *19*, 403.
- [15] K. Harrass, R. Kruger, M. Moller, K. Albrecht, J. Groll, *Soft Matter* **2013**, *9*, 2869.
- [16] M. Albrecht, G. van Koten, *Angew. Chem. Int. Ed.* **2001**, *40*, 3750.
- [17] D. Xu, S. L. Craig, *Macromolecules* **2011**, *44*, 5465.
- [18] W. C. Yount, D. M. Loveless, S. L. Craig, *Angew. Chem. Int. Ed.* **2005**, *44*, 2746.
- [19] W. C. Yount, D. M. Loveless, S. L. Craig, *J. Am. Chem. Soc.* **2005**, *127*, 14488.
- [20] E. A. Appel, J. del Barrio, X. J. Loh, O. A. Scherman, *Chem. Soc. Rev.* **2012**, *41*, 6195.
- [21] We report compression rate in velocity due to slight variations in height between samples. For reference, the height of the samples generally fall between 1.6 and 1.8 mm.
- [22] Y. Chen, A. J. H. Spiering, S. Karthikeyan, G. W. M. Peters, E. W. Meijer, R. P. Sijbesma, *Nat. Chem.* **2012**, *4*, 559.
- [23] E. Ducrot, Y. Chen, M. Bulters, R. P. Sijbesma, C. Creton, *Science* **2014**, *344*, 186.
- [24] J. P. Gong, *Soft Matter* **2010**, *6*, 2583.
- [25] X. Zhao, *Soft Matter* **2014**, *10*, 672.
- [26] K. R. Shull, *Nature* **2012**, *489*, 36.
- [27] K. J. Henderson, T. C. Zhou, K. J. Otim, K. R. Shull, *Macromolecules* **2010**, *43*, 6193.
- [28] W.-C. Lin, W. Fan, A. Marcellan, D. Hourdet, C. Creton, *Macromolecules* **2010**, *43*, 2554.
- [29] R. P. Sijbesma, F. H. Beijer, L. Brunsveld, B. J. B. Folmer, J. H. K. K. Hirschberg, R. F. M. Lange, J. K. L. Lowe, E. W. Meijer, *Science* **1997**, *278*, 1601.
- [30] E. A. Appel, F. Biedermann, U. Rauwald, S. T. Jones, J. M. Zayed, O. A. Scherman, *J. Am. Chem. Soc.* **2010**, *132*, 14251.
- [31] Y. Chen, A. M. Kushner, G. A. Williams, Z. Guan, *Nat. Chem.* **2012**, *4*, 467.
- [32] D. C. Tuncaboylu, M. Sari, W. Oppermann, O. Okay, *Macromolecules* **2011**, *44*, 4997.
- [33] P. Cordier, F. Tournilhac, C. Soulie-Ziakovic, L. Leibler, *Nature* **2008**, *451*, 977.
- [34] A. A. Griffith, *Philos. Trans. R. Soc. London, Ser. A* **1921**, *221*, 163.
- [35] J. Bastide, L. Leibler, *Macromolecules* **1988**, *21*, 2647.
- [36] A. Cristiano, A. Marcellan, B. J. Keestra, P. Steeman, C. Creton, *J. Polym. Sci., Part B: Polym. Phys.* **2011**, *49*, 355.
- [37] A. N. Gent, *Langmuir* **1996**, *12*, 4492.